and successful. AutoDock 4.0, combines energy evaluation through grids of affinity potential employing various search algorithms to find the suitable binding position for a ligand on a given protein. The structure of ligand molecule (compound I) was analyzed using ChemDraw Ultra 8.0 by CambridgeSoft Corporation (Cambridge Scientific Computing, Inc.), USA. 3D, coordinates were prepared using PRODRG server. The protein structure file (Protein Data Bank [PDB]: 2I0J and 2YJD) taken from PDB (www.rcsb.org/pdb) was edited by removing the heteroatoms, adding C-terminal oxygen. All torsions were allowed to rotate during docking. Steepest descent methods were applied for minimization, using default parameters. While docking, polar hydrogen's were added to ligand using the hydrogen's module in AutoDock tool and thereafter, Kollman united atom partial charges were assigned. Docking to ligand was carried out with standard docking protocol on the basis a population size of 150 randomly placed individuals; a maximum number of 2.5 × 107 energy evaluations, a mutation rate of 0.02, a crossover rate of 0.80 and an elitism value of 1. Fifteen independent docking runs were carried out for ligand and results were clustered according to the 1.0 Å rmsd criteria. The grid maps representing the proteins were calculated using auto grid and grid size was set to 60 × 60 × 60 points with grid spacing of 0.375 Å. The active site, i.e., Arg-394 and Glu-305 in the protein interacts with ligand of the substrate and gives increase to the catalytic activity to test ligand that helps in determining the binding pattern of the ligand to the active site of the ER. The docking results were interpreted according to the.pdb file. We have used the coordinates of the minimum energy run created in the.dlg which was determined using the rmsd table created in the.dlg file itself. The coordinate of the docked protein along with compound I was visualized using UCSF chimera within 6.5 Å region.

Anti-cancer activity (*in vitro*)

MCF-7, MDA-MB-231, PC-3, and DU-145 cells used in this study were obtained from the American Type Culture Collection, USA and were routinely maintained in Dulbecco's Modified Eagle Medium (Sigma-Aldrich) supplemented with 10% fetal bovine serum (Merck) and 1% antibiotic and antimycotic solution (Merck) at 37°C in a humidified incubator with 5% CO_2. All stock solution of compounds (NCCL and compound I) was prepared in cell culture grade DMSO and stored in −20°C. Compounds were diluted in culture media before use in experiments. Cell viability was assessed using MTT assay, which is based on the reduction of MTT by mitochondrial dehydrogenases of viable cells to form a purple formazan product. In brief, MCF-7, MDA-MB-231, PC-3, and DU-145 cells (5×10^3/well) were plated in 96-well plates. After incubating for overnight, the cells were treated with different concentrations (200, 100, 50, 25, 12.5, and 6.25 µg/ml, in triplicates) of NCCL and compound I for 48 h. Subsequently, 10 µL of MTT (10 mg/mL) was added to each well and incubated for 3 h. The MTT formazan formed by viable cells was dissolved in 100 µL of DMSO and shaken for 10 min. The absorbance was measured at 540 nm on an ELISA reader. Each test was repeated at least 3 times. The concentration of the compound which gives the 50% growth inhibition value corresponds to IC_{50}, calculated using GraphPad Prism 5 by GraphPad Software Inc.

RESULTS

HPLC fingerprinting of blank ACN, HM, and NCCL was done and retention time and % peak area of HM and NCCL at 220 nm and 254 nm is given in Table 1.

Compound I [Figure 1], was isolated from NCCL by preparative HPLC. The fractions containing marker compound were separated and concentrated under vacuum. The marker compound, I was characterized as 7,7-dimethyl-5-(2-p-tolylpropyl)-6,7-dihydro-1,3,4-oxadiazepin-2-amine employing different spectral techniques such as FTIR, ^1H and ^{13}C NMR, Mass. The purity of compound I was checked by TLC and HPLC and was found >99% pure.

Table 1: Retention time and percentage peak area of herbal medicament and NCCL at 220 and 254 nm

HM				NCCL			
220 nm		254 nm		220 nm		254 nm	
Rt	% area	Rt	% area	Rt	% area	Rt	% area
1.967	0.04	1.233	0.02	1.659	0.21	1.722	0.17
2.105	0.15	1.518	0.02	2.032	0.06	2.143	1.32
2.478	2.07	1.710	0.11	2.259	0.07	2.388	0.98
3.374	1.99	1.990	0.14	2.513	1.39	2.570	1.68
3.850	3.64	2.223	0.45	2.801	0.38	2.795	2.35
4.243	0.04	2.481	6.23	3.095	2.47	3.163	2.90
4.601	1.67	3.168	0.30	3.365	3.27	3.719	11.44
5.134	0.79	3.428	0.64	3.772	2.08	4.119	1.32
5.710	0.04	3.841	3.51	4.146	0.94	4.467	50.34
5.941	0.04	4.245	0.54	4.468	50.25	5.091	0.99
6.153	0.44	4.622	1.30	5.093	13.91	5.258	1.08
6.953	2.13	4.783	0.88	5.836	0.21	5.422	1.42
8.796	0.29	5.159	0.91	6.570	0.76	5.840	1.51
9.236	0.17	6.152	2.72	7.331	1.02	6.461	2.02
9.836	71.45	6.716	1.02	7.835	7.09	6.971	0.89
12.030	0.07	8.870	0.80	8.983	0.06	7.840	0.74
12.590	3.45	9.837	50.04	9.359	0.09	8.276	0.17
14.269	10.72	12.069	0.03	9.832	0.08	9.348	0.70
17.681	0.25	12.708	0.80	10.305	0.78	9.827	0.23
18.703	0.11	14.290	12.53	10.884	0.04	10.286	1.84
23.895	0.32	14.654	11.41	11.311	0.33	11.202	0.16
29.328	0.12	17.873	0.10	12.042	0.57	12.728	1.30
-	-	18.720	4.23	12.639	1.74	14.969	0.02
-	-	21.826	0.06	14.164	0.10	15.441	0.32
-	-	22.473	1.15	15.428	0.28	16.042	0.25
-	-	29.177	0.07	16.001	0.16	17.325	0.10
-	-	-	-	17.401	1.63	21.849	0.13
-	-	-	-	21.861	0.54	26.125	2.10
-	-	-	-	23.798	0.14	29.146	11.40
-	-	-	-	26.128	1.41	29.868	0.15
-	-	-	-	29.146	7.95	-	-

Rt: Retention time; HM: Herbal medicament

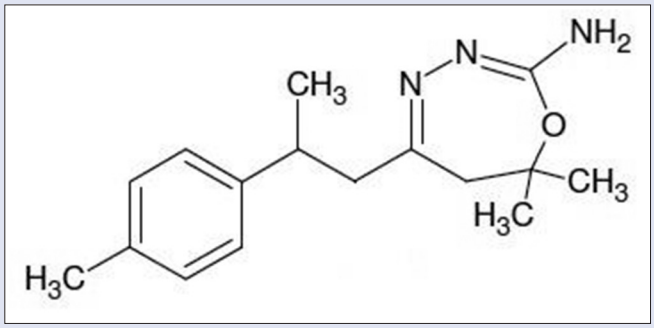

Figure 1: Structure of 7,7 dimethyl 5 (2 p tolylpropyl) 6, 7 dihydro 1,3,4 oxadiazepin 2 amine (compound I)

Infrared data

IR (KBr) (cm^{-1}): 3411.7, 3015.2, 1667.2, 1564.5, 1514.7, 1448.0, 1216.1, 1054.7, 759.7, 669.1, 544.7.

Nuclear magnetic resonance data

^{1}H NMR (400 MHz, DMSO-d_6): δ 7.13 (d, 2H, J = 7.68), δ 7.08 (d, 2H, J = 7.56), δ 5.93 (S, 2H), δ 3.01 (dd, 1H, J = 6.90), δ 2.5 (m, 4H), δ 2.24 (s, 3H), δ 1.31 (s, 3H), δ 1.23(s, 3H), δ 1.18 (d, 3H, J = 6.72).

^{13}C NMR (400 MHz, DMSO-d_6): δ 155.41, 153.28, 142.96, 135.04, 128.86, 126.69, 61.66, 50.85, 37.98, 36.55, 26.00, 25.78, 22.29, 20.59.

Mass data

Mass: M/z 274.5 (M^++1), 275.6 (M^++2), HRMS m/z 274.1932 (M^++1), 275.1956 (M^++2).

Elemental analysis data

Anal. Calc. for $C_{17}H_{25}N_3O$: C 71.04, H 8.77, N 14.62; Found: C 68.179, H 8.517, N 13.247.

The binding poses in the docking studies are energetically favorable. The *in vitro* anticancer activity of NCCL and compound I was checked against four cancer cell lines namely MCF-7, MDA-MB-231, PC-3 and DU-145 at concentrations of 200, 100, 50, 25, 12.5, and 6.25 μg/ml, in triplicates. IC_{50} values in μM against various cell lines are given in Table 2.

Table 2: IC_{50} values of NCCL and compound I in μM against various cell lines

Compound IC_{50} (μM)	MCF-7	MDA-MB-231	PC-3	DU-145
NCCL	2.093	8.57	9.24	10.78
I	17.28	>20	19.82	>20
TAM	5.5	11.4	10	5.5
Epirubicin	3.7	5.6	5.7	9.9

TAM: Tamoxifen

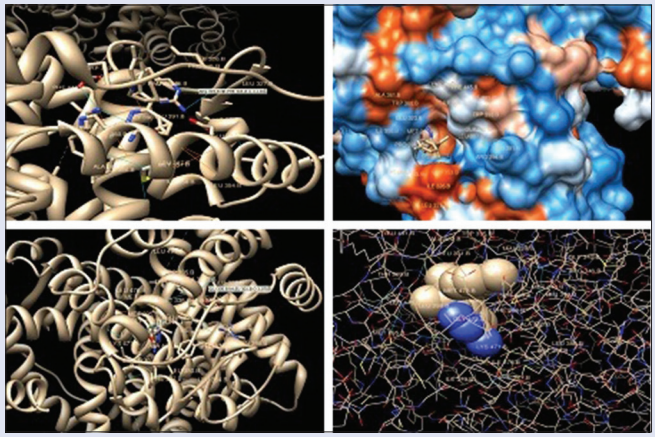

Figure 2: Docking of compound I into active site of estrogen receptors (estrogen receptor-α and estrogen receptor-β) showing bonding with the amino acids in the active pockets

DISCUSSION

NCCL was prepared from HM which is a hexane soluble fraction of *C. longa*. Compound I, 7, 7-dimethyl-5-(2-p-tolylpropyl)-6, 7-dihydro-1,3,4-oxadiazepin-2-amine ($C_{17}H_{25}N_3O$), was isolated from NCCL by preparative HPLC. Compound I is characterized using 1D/2D NMR, mass spectroscopy (MS) and FT-IR techniques. The base peak in electrospray ionization-MS was found at M^++1 (274.5). In IR spectra, a band at 3411.7 cm^{-1} indicated the N-H stretching of amine group, a strong band at 1514 cm^{-1} indicated the presence of conjugation in cyclic imine (C=N-). The presence of azine group (C=N-N=C) and amine group (–NH_2) is indicated at by the presence of peaks at 1564 and 759 cm^{-1}, respectively. Peaks at 1448 and 1054 cm^{-1} indicated the presence of methyl groups (R-CH_3) and methyl benzene (C_6H_5-CH_3), respectively. Cyclic ether (-C-O-C-) and cyclic alkene with internal double bonds are indicated by peak at 1216 and 669 cm^{-1}, respectively. Peak at 544 cm^{-1} indicated the presence of monobranched alkane. ^{1}H NMR spectra of compounds I gave a singlet between 2.24 and 1.18 ppm which indicated the presence of three protons of the methyl group (–CH_3). Aiphatic-CH is indicated by the peak at 3.01 ppm. Broad singlet at 5.93 ppm was found indicating two protons attached to the nitrogen atom (–NH_2). Peaks between 7.13 and 7.08 ppm indicated the presence of protons of the aromatic ring of compound. ^{13}C spectra clearly supported the results obtained from ^{1}H NMR spectra and also justified the number of carbon atoms in corresponding compounds.

After the achievement of isolation and characterization of the compound I, we performed *in silico* studies. To expose the specificity of the ERs (Er-α and Er-β) toward the target compounds, docking approach was carried out. Docking was used to predict the binding orientation of compound I to its protein target to in turn predict the affinity and activity of compound I which includes docking of ligand to a set of grids describing the target protein. The target compound I was docked into the nucleotide-binding pocket of the ERs alpha and beta (PDB: 2I0J and 2YJD). A Lamarckian genetic algorithm method, implemented in the program AutoDock 4.0, was employed. The docking of the ligand molecule (I) reveals that the inhibitor compound is exhibiting the bonding with one or the other amino acids such as Arg-394 and Glu-305 in the active pockets [Figure 2]. Compound no. I had shown the minimum binding energy of −8.72 and −9.31 kcal/mol with inhibition constant 405.35 and 149.38, respectively. The compound I had shown favorable drug-like properties and follow the Lipinski's rule of 5 with additional parameters predicted by Molsoft. The drug-likeness score of compound I is −0.82 with approximate molecular weight of 287, log *P* value of 4.11, log S value of −3.97, prostate-specific antigen value of 49.57, 3 hydrogen bond acceptors and 2 hydrogen bond donors.

With *in silico* results in hand, it was thought worthwhile to do *in vitro* studies to support the *in silico* studies. The *in vitro* anticancer activity of NCCL and compound I was checked against cancerous (breast and prostate) cells at different concentrations (200, 100, 50, 25, 12.5, and 6.25 μg/ml, in triplicates). The cell lines used in this investigation include MCF-7, MDA-MB-231, PC-3, and DU-145. NCCL significantly inhibited the proliferation of breast cancer cell MCF-7 (IC_{50}~2.1 μM), and MDA-MB-231 (IC_{50}~8.5 μM) as well as prostate cell lines PC-3 (IC_{50}~9.2 μM) and DU-145 (IC_{50}~10.7 μM) [Table 2].

CONCLUSION

We have reported for the first time, the synthesis of a novel chemically modified bioactive fraction from HM (NCCL) and isolation of a novel marker compound I, 7,7-dimethyl-5-(2-p-tolylpropyl)-6, 7-dihydro-1,3,4-oxadiazepin-2-amine (reaction product of ar-turmerone with semicarbazide). Their inhibitory effects on ERs were evaluated using *in silico* followed by *in vitro* studies. A molecular docking study has revealed that compound I have minimum binding energy with favorable drug-likeness scores and may be considered a good estrogen blocker. The order of NCCL sensitivity was MCF-7 cells > MDA-MB-231 cells and PC-3 > DU-145 cell. NCCL fraction having residual components induces more cell death than compound I alone. NCCL turned out to be a potent anticancer agent over compound I against these four cancer cell lines and has emerged as a promising alternative to the marketed TAM.

Further work is progress in our laboratory to evaluate their *in vivo* anticancer potential and in-depth mechanistic aspects.

Financial support and sponsorship

Nil.

Conflicts of interest

There are no conflicts of interest.

REFERENCES

1. Stratton CF, Newman DJ, Tan DS. Cheminformatic comparison of approved drugs from natural product versus synthetic origins. Bioorg Med Chem Lett 2015;25:4802-7.
2. Prasad S, Aggarwal BB. Turmeric, the Golden Spice: From Traditional Medicine to Modern Medicine. 2nd ed. Boca Raton, FL: CRC Press, Taylor and Francis; 2011.
3. Sandur SK, Pandey MK, Sung B, Ahn KS, Murakami A, Sethi G, *et al*. Curcumin, demethoxycurcumin, bisdemethoxycurcumin, tetrahydrocurcumin and turmerones differentially regulate anti-inflammatory and anti-proliferative responses through a ROS-independent mechanism. Carcinogenesis 2007;28:1765-73.
4. Dohare P, Garg P, Sharma U, Jagannathan NR, Ray M. Neuroprotective efficacy and therapeutic window of curcuma oil: In rat embolic stroke model. BMC Complement Altern Med 2008;8:55.
5. Prakash P, Misra A, Surin WR, Jain M, Bhatta RS, Pal R, *et al*. Anti-platelet effects of Curcuma oil in experimental models of myocardial ischemia-reperfusion and thrombosis. Thromb Res 2011;127:111-8.
6. Rana M, Reddy SS, Maurya P, Singh V, Chaturvedi S, Kaur K, *et al*. Turmerone enriched standardized *Curcuma longa* extract alleviates LPS induced inflammation and cytokine production by regulating TLR4–IRAK1–ROS–MAPK–NFκB axis. J Funct Foods 2015;16:152-63.
7. Apisariyakul A, Vanittanakom N, Buddhasukh D. Antifungal activity of turmeric oil extracted from *Curcuma longa* (Zingiberaceae). J Ethnopharmacol 1995;49:163-9.
8. Negi PS, Jayaprakasha GK, Jagan Mohan Rao L, Sakariah KK. Antibacterial activity of turmeric oil: A byproduct from curcumin manufacture. J Agric Food Chem 1999;47:4297-300.
9. Tripathi AK, Prajapati V, Verma N, Bahl JR, Bansal RP, Khanuja SP, *et al*. Bioactivities of the leaf essential oil of *Curcuma longa* (var. ch-66) on three species of stored-product beetles (Coleoptera). J Econ Entomol 2002;95:183-9.
10. Roth GN, Chandra A, Nair MG. Novel bioactivities of *Curcuma longa* constituents. J Nat Prod 1998;61:542-5.
11. Jayaprakasha GK, Jena BS, Negi PS, Sakariah KK. Evaluation of antioxidant activities and antimutagenicity of turmeric oil: A byproduct from curcumin production. Z Naturforsch C 2002;57:828-35.
12. Ray M, Pal R, Singh S, Khanna NM. Herbal Medicaments for the Treatment of Neurocerebrovascular Disorders. US Patent No. 6991814; 31 January, 2006.
13. Simon A, Allais DP, Duroux JL, Basly JP, Durand-Fontanier S, Delage C. Inhibitory effect of curcuminoids on MCF-7 cell proliferation and structure-activity relationships. Cancer Lett 1998;129:111-6.
14. Shao ZM, Shen ZZ, Liu CH, Sartippour MR, Go VL, Heber D, *et al*. Curcumin exerts multiple suppressive effects on human breast carcinoma cells. Int J Cancer 2002;98:234-40.
15. Aggarwal BB, Kumar A, Bharti AC. Anticancer potential of curcumin: Preclinical and clinical studies. Anticancer Res 2003;23:363-98.
16. Naksuriya O, Okonogi S, Schiffelers RM, Hennink WE. Curcumin nanoformulations: A review of pharmaceutical properties and preclinical studies and clinical data related to cancer treatment. Biomaterials 2014;35:3365-83.
17. Reddy BS, Banerjee R. 17Beta-estradiol-associated stealth-liposomal delivery of anticancer gene to breast cancer cells. Angew Chem Int Ed Engl 2005;44:6723-7.
18. Carruba G. Estrogen and prostate cancer: An eclipsed truth in an androgen-dominated scenario. J Cell Biochem 2007;102:899-911.
19. Baumann CK, Castiglione-Gertsch M. Estrogen receptor modulators and down regulators: Optimal use in postmenopausal women with breast cancer. Drugs 2007;67:2335-53.
20. Lipinski CA. Drug-like properties and the causes of poor solubility and poor permeability. J Pharmacol Toxicol Methods 2000;44:235-49.
21. Lipinski CA, Lombardo F, Dominy BW, Feeney PJ. Experimental and computational approaches to estimate solubility and permeability in drug discovery and development settings. Adv Drug Deliv Rev 2001;46:3-26.
22. Vistoli G, Pedretti A, Testa B. Assessing drug-likeness – What are we missing? Drug Discov Today 2008;13:285-94.
23. Narender T, Sukanya P, Sharma K, Bathula SR. Apoptosis and DNA intercalating activities of novel emodin derivatives. RSC Adv 2013;3:6123-31.
24. Dwivedi AK, Naqvi A, Malasoni R, Rana M, Pandey RR, Srivastava A, *et al*. Indian Patent Application No. 1940/DEL/2014, Published 31 Aug 2016.